

# Shape-memory nanoparticles from inherently non-spherical polymer colloids

ZHONGQIANG YANG<sup>1</sup>, WILHELM T. S. HUCK<sup>2\*</sup>, STUART M. CLARKE<sup>3</sup>, ALI R. TAJBAKHSH<sup>4</sup> AND EUGENE M. TERENTJEV<sup>4</sup>

<sup>1</sup>Melville Laboratory for Polymer Synthesis, Department of Chemistry, University of Cambridge, Lensfield Road, Cambridge CB2 1EW, UK

<sup>2</sup>The Nanoscience Centre, J J Thomson Avenue, Cambridge CB3 0FF, UK

<sup>3</sup>BP Institute, University of Cambridge, Madingley Rise, Madingley Road, Cambridge CB3 0EZ, UK

<sup>4</sup>Cavendish Laboratory, University of Cambridge, Madingley Road, Cambridge CB3 0HE, UK

\*e-mail: wtsh2@cam.ac.uk

Published online: 15 May 2005; doi:10.1038/nmat1389

Samples of polymeric materials generally have no intrinsic shape; rather their macroscopic form is determined by external forces such as surface tension and memory of shear (for example, during extrusion, moulding or embossing). Hence, in the molten state, the thermodynamically most stable form for polymer (nano)particles is spherical. Here, we present the first example of polymer nanoparticles that have an intrinsic non-spherical shape. We observe the formation of high-aspect-ratio ellipsoidal polymer nanoparticles, of controlled diameter, made from main-chain liquid crystalline polymers using a mini-emulsion technique. The ellipsoidal shape is shown to be an equilibrium (reversible) characteristic and a direct result of the material shape memory when a liquid crystal nanoparticle is in its monodomain form.

Liquid crystalline polymers and elastomers have received considerable attention because of their remarkable macroscopic properties that result from the alignment of rigid, rod-like segments at the monomer level coupled to the average conformation of polymer chains<sup>1,2</sup>. Among the many intriguing effects demonstrated by these and related materials are ‘shape memory’ leading to mechanical actuation (the conversion of light or thermal energy into mechanical energy)<sup>2,3</sup>, and ‘soft elasticity’ (the ability of an elastic medium with microstructure to deform without a stress response)<sup>2,4</sup>.

Here we study the properties of main-chain liquid crystalline polymer (MCLCP) nanoparticles. We demonstrate, for the first time, that within a certain range of particle sizes their shape becomes naturally ellipsoidal, with a significant aspect ratio. This shape is determined by the quasi-equilibrium shape memory of entangled MCLCP and changes reversibly back to spherical on heating the polymers into the isotropic phase. The ability to fix the anisotropic shape of the nanoparticles and reversibly change it by stimuli such as temperature or light (in photochromic materials) makes this effect important for nanotechnological applications such as nanoactuators.

Macroscopically, traditional amorphous polymeric materials have no preferred shape. Individual polymer molecules generally adopt an isotropic ‘random coil’ conformation in the melt or solution. Hence polymer particles (with sizes ranging from several nanometres to several micrometres) are spherical in shape as a result of minimizing surface tension. Over the past decades, research has gone into assembling such particles into colloidal suspensions with a variety of interparticle interactions, and the formation of colloidal crystals, with applications such as photonic crystals<sup>5,6</sup>. The assembly of regularly shaped non-spherical particles would greatly expand these and many other applications<sup>7</sup>. Submicrometre particles of inorganic materials ranging from needles to spheres can be synthesized by carefully controlled crystal growth conditions<sup>8,9</sup>, or by anisotropic deformation under ion irradiation of certain amorphous inorganic materials<sup>10</sup>. Non-spherical polymeric particles have been prepared

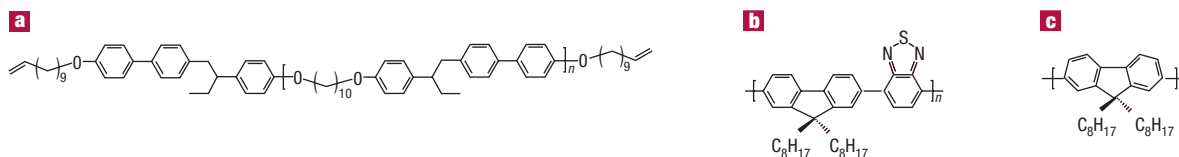


**Figure 1** Chemical structures of the polymers used in this study. **a**, Main-chain polyether ( $T_g$  28.1 °C,  $T_{NI}$  95.1 °C,  $M_w$  13,000); **b**, poly(9,9-dioctylfluorene-co-benzothiadiazole) (F8BT) ( $T_g$  121.8 °C,  $T_{cryst}$  152.6 °C,  $T_m$  240.2 °C,  $M_w$  203,000); **c**, poly(9,9-dioctylfluorene) (PFO) ( $T_g$  78.0 °C,  $T_{cryst}$  98.6 °C,  $T_m$  149.0 °C,  $M_w$  79,000).

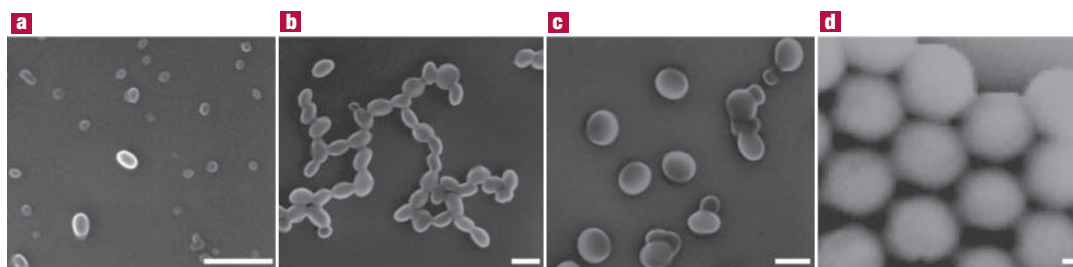


**Figure 2** SEM images of main-chain polyether nanoparticles with different morphologies and sizes. **a–d**, The aspect ratio of main-chain polyether particles changes with size. **a**, Aspect ratio of 1.0 in the case of 28-nm spheres (small particles); **b**, 1.5 for 140-nm-long ellipsoids; **c**, 1.2 for 200-nm-long ellipsoids; and **d**, back to 1.0 for 1,000-nm spheres. The white bar represents 200 nm in each case.

previously, but only by elaborate multistep procedures<sup>11,12</sup>, and they have to be frozen in their non-equilibrium shapes by the glassy nature of the polymers<sup>13</sup>. The approach and the particles that we describe below provide the first example of polymer materials with intrinsic shape selection (that is, their equilibrium shape is spontaneously determined by the translation of local molecular structure and anisotropy into meso- and macroscopic length scales). Our nanoparticles prepared from MCLCPs spontaneously adopt prolate ellipsoidal shapes with high aspect ratio. In addition, this shape can be controlled and manipulated by changing the underlying nematic order (by altering the temperature, as in our reported experiments, or by other means such as ultraviolet irradiation).

In this work we used the polymers shown in Fig. 1, but we will focus our attention on particles formed from the main-chain polyether<sup>14</sup> (Fig. 1a), which has well-characterized properties and reasonably accessible glass ( $T_g$ ) and nematic ( $T_{NI}$ ) transition temperatures, ensuring that the particles are in equilibrium. However, we also used two different polymers, F8BT and PFO, shown in Fig. 1b and c, which have much higher  $T_g$  and clearing point (transition into isotropic state), making them glassy at room temperature. All polymers have been reported to display a liquid crystal phase<sup>15</sup>. No values for the clearing points of F8BT and PFO are known, as these are high and often accompanied by decomposition. Polymer nanoparticles were prepared by the mini-emulsion route<sup>16</sup>. By varying the relative amounts of surfactant and polymer, different sizes of particles can be obtained. Briefly, the MCLCPs were dissolved in chloroform and mixed with water and surfactant. After ultrasonication for 5 min, a stable mini-emulsion formed and evaporation of chloroform resulted in a stable suspension of MCLCP nanoparticles, with typical sizes in the range 30–150 nm. This relatively straightforward preparation technique gives moderately polydisperse particles which are sufficient for our present work. In future work, we will control the polydispersity to a greater extent by improving the conditions for the mini-emulsion technique. Typical nanoparticles obtained using the main-chain polyether are presented in Fig. 2. Clearly, particles

in the size range 100–200 nm as shown in Fig. 2b and c are not spherical but prolate ellipsoids. Similar preparation procedures used on non-liquid-crystalline polymers such as TFB and polystyrene (see Supplementary Information) gave similarly sized but spherical particles (as classical colloid science dictates). This result clearly indicates that the formation of ellipsoidal particles is a specific property of the liquid crystalline polymer and does not result from other factors such as surfactant behaviour. Additional studies confirmed that the nature of the surfactant (cationic or anionic) has no apparent influence on the particle shape (see Supplementary Information for different surfactants used).

When studying the size anisotropy in more detail, a clear relationship is observed between particle size and the aspect ratio (major versus minor axis) of main-chain polyether ellipsoids. The scanning electron microscope (SEM) images in Fig. 2 show that the particle morphology changes from spherical to ellipsoidal and to spherical again. When the particle size is below 30 nm (Fig. 2a, small particles), particles tend to be spherical. With increasing size, particles show an ellipsoidal shape with aspect ratio of about 1.5, with major and minor axes around 138 nm and 90 nm respectively. The aspect ratio decreases to 1.2 when the particle size increases to 200 nm, and particles become completely spherical when the diameter reaches 1,000 nm. The results show that there is a pronounced variation in behaviour with the average size of the particles. In outline the trend is as follows: small particles are spherical, intermediate-sized particles are ellipsoidal and larger particles are again spherical.

The ellipsoidal shape of main-chain polyether nanoparticles must reflect the current state of nematic ordering in the underlying polymer chains, which must have an equilibrium conformation that is not an isotropic, random coil arrangement but a prolate ellipsoid. Accordingly, heating the nematic polymers above the nematic to isotropic transition temperature  $T_{NI}$  should turn the ellipsoidal particles into spherical ones. This temperature effect was investigated by cycling the temperature of the particles through their  $T_{NI}$  by annealing and cooling a suspension of main-chain

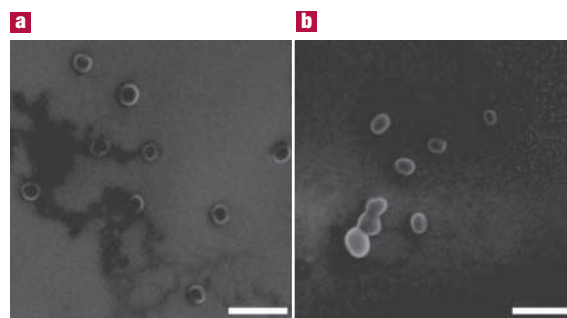


**Figure 3** SEM images of main-chain polyether nanoparticles. Particles are shown after being annealed at 101 °C for 40 s and (a) quickly quenched in liquid nitrogen; (b), slowly cooled to room temperature. The white bar represents 200 nm.

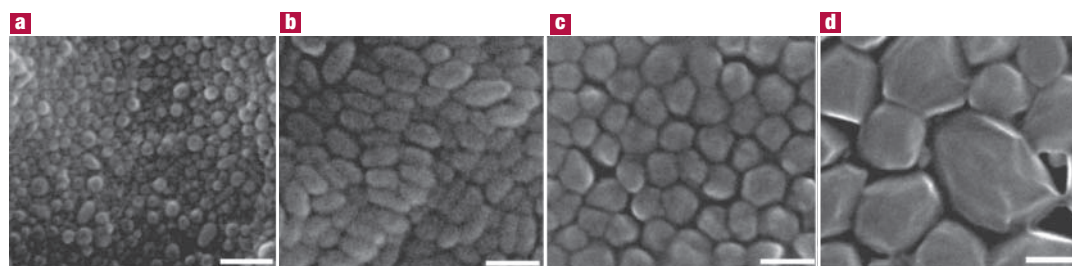


**Figure 4** SEM images of F8BT nanoparticles with different shapes and sizes. The apparent trend of shape dependence on particle size confirms that seen in MCLCP. a–c, The F8BT nanoparticle shape changes from (a) spheres (30 nm) to (b) ellipsoids and back to (c) spheres (70 nm). The aspect ratio varies from 1.0 to 2.2 and to 1.0 correspondingly. d, Irregular particles with size larger than 120 nm. The white bar represents 100 nm.

polyether nanoparticles in water. The suspension was annealed for 40 s at 101 °C and then rapidly quenched in liquid nitrogen (not allowing the equilibrium nematic order, and the associated particle shape anisotropy, to develop). Figure 3a shows that nanoparticles frozen in their high-temperature conformation are spherical. At 101 °C, the main-chain polyether is in the isotropic phase. No chain alignment inside the particles takes place to counteract surface tension, and particles change from ellipsoids to spheres as in all classical colloids. However, when the annealed suspension is allowed to cool to room temperature slowly, the nanoparticles return to a non-spherical shape (Fig. 3b), demonstrating that the shape change is a reversible process and that the particle shape is their equilibrium, intrinsic property. It should be noted that the  $T_g$  of this polymer is 28.1 °C, but that the ellipsoidal shape is persistent up to the clearing temperature ( $T_{NI} \approx 95$  °C). This demonstrates that even when the polymer melt has sufficient mobility, the particles do not deform, and the ellipsoidal shape is indeed the equilibrium shape.

A theoretical model explaining these observations, based on the physics of the underlying liquid crystalline polymer, will be presented in detail elsewhere. This will include an explanation of the subtle variations of aspect ratio with particle size and material, as suggested by our results. Here we present a qualitative picture that could account for the observed behaviour. There is a clear parallel between our findings and the equilibrium shape-memory properties of nematic elastomers (see ref. 2 for details). However, there are three challenges to address. (i) The polymers forming the nanoparticles are not deliberately crosslinked; why then does the material behave like a shape-memory nematic elastomer? (ii) What determines the lower ‘critical size’ below which the particles are spherical? (iii) What happens above the

upper ‘critical size’, when the particles become spherical again before becoming irregular?

First, let us deal with the issue of effective crosslinking, which is the central point of this argument. We propose that the origin of the observed effects lies in the main-chain nature of these nematic polymers. Such chains are known to fold into hairpins in the nematic phase<sup>17</sup> and the size of hairpins is particularly small (localization effect) in chains that contain rigid rod segments connected with flexible spacers, as in our main-chain polyethers. In the dense melt, the lateral mobility of chain segments is restricted by the neighbours, which effectively confine each individual chain in a narrow tube with only the reptation motion along the tube remaining as the mechanism of equilibration: viscoelastic polymer melts are very far in their mechanical properties from an ordinary liquid<sup>18</sup>. Typical tube diameters have been reported in the range of 2–4 nm. When the reptation tube that confines the motion of a MCLCP in the nematic phase is folded into a corresponding hairpin, there is a regime of sufficiently small tube diameter and hairpin radius at which the rigid-rod molecular moiety will not be able to negotiate the turn, and chain reptation effectively freezes (chain diffusion ceases altogether). In this new dynamical regime, only present in hairpin-folded main-chain nematic polymers, thermal reptation motion is only allowed between hairpins, which therefore play the role of effective network crosslinks. The effective rubber modulus of such a dynamically constrained polymer melt is, accordingly, proportional to the hairpin density, which is a known function of nematic order parameter<sup>2,18</sup>. It has been experimentally demonstrated that the restricted chain mobility of MCLCP melt in the nematic phase leads to physical properties closely resembling those of permanently crosslinked nematic rubber<sup>19,20</sup>. We believe this is also responsible

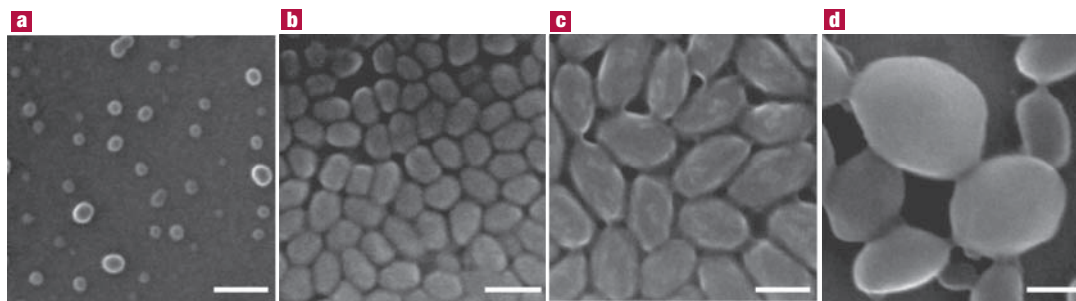


**Figure 5** SEM images of PFO nanoparticles with different shapes and sizes. **a–c**, The aspect ratios of (a) spheres (25 nm), (b) ellipsoids and (c) ellipsoids are 1.0, 1.45 and 1.8 respectively. **d**, The nanoparticles are irregular in shape when the size is over 200 nm. The white bar represents 100 nm.

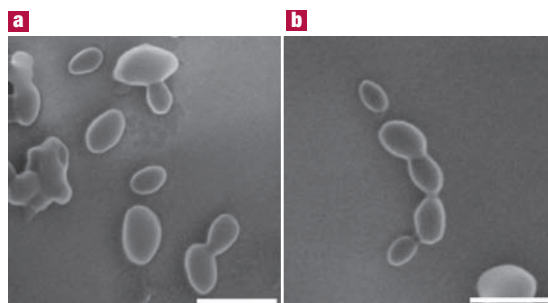


**Figure 6** SEM images of annealed PFO nanoparticles. **a**, After annealing the suspension at 101 °C for 40 s and subsequent quenching in liquid nitrogen; **b**, after annealing at 101 °C for 40 s and slowly cooling to room temperature. The white bar represents 100 nm.

for ‘locking’ the ellipsoidal shape memory of MCLCP particles, and ultimately of other nematic polymers.

Let us now consider the lower size limit on the ellipsoidal range. As the particles become smaller the relative contribution of the surface compared with the volume increases significantly. Interfacial tension will always be present as the energy penalty and will therefore increasingly drive the particles to be spherical as they become smaller. The particles at this size range will be expected to be nematic monodomain (see later) and hence the equilibrium shape, without taking into account the surface tension, would be prolate ellipsoidal. The interfacial tension will need to elastically distort the equilibrium ellipsoids back to spheres as the particles reduce in size. Elementary calculations comparing the elastic energy cost (reflected in the effective rubber-elastic modulus,  $\mu$ ) of distorting the ellipsoids with the change in interfacial energy (tension  $\gamma$ ) indicate that the lower critical radius  $R$  scales as:

$$R \propto \gamma/\mu$$

A typical value of the modulus of these materials is  $10^5$  to  $10^6$  N m $^{-2}$ . This estimate, and the whole concept of a ‘rubber modulus’, relies on the effective constraints on chain reptation motion imposed by tightly folded hairpins. The interfacial tension of mini-emulsions has been determined by Landfester to be  $\sim 6 \times 10^{-2}$  N m $^{-1}$  for a number of organic materials with sodium dodecylsulphate (SDS) as a surfactant<sup>21</sup>. Hence the lower critical radius below which we expect spheres is about 60 nm. Considering the qualitative level of this estimate, the order-of-magnitude agreement with our observations is very satisfactory.

The upper size limit of the ellipsoidal range has to be explained by referring to the characteristic size of aligned nematic domains in a main-chain polyether melt. To show an ellipsoidal shape that depends on the order parameter, the particles need to be monodomain, uniformly aligned nematic liquid crystals. But it is well known that the macroscopically polydomain state is the equilibrium in nematic elastomers, because of the effect of quenched orientational disorder imposed by network crosslinks<sup>22</sup>. In our MCLCP system, the tightly folded hairpins present exactly the same quasi-equilibrium effect as has been demonstrated in a study of polydomain melts<sup>19,20</sup>. Hence the upper limit on the ellipsoidal range is set by the natural domain size of the liquid crystalline polymers,  $\xi_D$ . If the particle is smaller than a typical domain size it will be an orientational monodomain and of ellipsoidal shape. If the particles are much bigger than a domain size  $\xi_D$ , then each will contain several domains in different orientations, resulting in a macroscopically isotropic, spherical shape. The domain size in a liquid crystal of this type has been shown<sup>2,22</sup> to be of the form

$$\xi_D = k^2/\rho g^2$$

where  $k$  is the Frank elastic constant for the polymer (a function of the material and the nematic order parameter),  $\rho$  represents a measure of the sources of quenched disorder in the system (hairpins in our case, whose density is also a function of nematic order) and  $g$  is the coupling energy between these disrupting regions and the director field (less is known about this parameter, although some estimates are given in the quoted literature). Previous work has shown that the typical domain size for liquid crystalline polymers of the type used here,  $\xi_D$ , is about



1  $\mu\text{m}$  or slightly less<sup>19</sup>. One has to bear in mind that the concept of aligned 'domains' due to the random quenched disorder is only a property of correlation functions—there are no uniform regions separated by sharp walls, instead there is simply a gradual loss of correlation in nematic director alignment over a distance  $\sim\xi_D$ . Therefore, our experimental observation that the 'upper critical size' of our particles is several times smaller than 1  $\mu\text{m}$  is still reasonable. In fact, we are encouraged by this crude estimate that the two characteristic sizes are in the right relation to each other and in the right order of magnitude. As part of the predictions produced by this model, we could say that the observed ellipsoidal shapes should not be observed in side-chain LCPs (owing to the absence of hairpin constraints). Of course, if one formed particles of weakly crosslinked nematic elastomer, they would show shape memory as well. From other studies<sup>19</sup> we know that the nematic domain size grows as the temperature rises towards  $T_{\text{NI}}$ . Accordingly, the upper critical size should become higher. It is interesting that the lower critical size (determined by the hairpin density, through the effective rubber modulus) should be a non-monotonic function of temperature: there are no hairpins near the nematic–isotropic transition, but equally the MCLCP chains in the melt would straighten more and thus reduce the hairpin density when the nematic order became very high at low temperatures.

To illustrate the generality of the formation of intrinsically non-spherical particles, we now present a range of particles prepared from two other liquid crystalline polymers, F8BT and PFO, best known in studies of semiconducting polymers. The results shown in Fig. 4 for F8BT again clearly illustrate the dependence of particle aspect ratio on average particle size, going from spherical particles for sizes below 30 nm to ellipsoidal shapes for larger diameters. Some of the largest anisotropy was observed in particles with  $\sim 40$  nm minor axis (maximum aspect ratio slightly over 2.0; major and minor axes of 78 nm and 36 nm, respectively). Some larger particles (around 120 nm) have irregular shapes, although this may be a result of deformation caused by drying on the surface while the scanning electron microscopy images were prepared.

PFO particles show a similar trend (Fig. 5): when the particles are very small, around 25 nm, surface tension apparently dominates and the particles are more or less spherical (aspect ratio 1.0). Slightly increasing the average particle size leads to ellipsoidal particles with an aspect ratio of 1.45 (63 nm major axis and 44 nm minor axis). Further increasing the particle size results in a further increase in aspect ratio to 1.8 (major axis 137 nm, minor axis 76 nm). The particles become irregular in shape when their size exceeds 200 nm.

Both PFO and F8BT are glassy at room temperature and one may question the arguments about their equilibrium shape. To prove that these ellipsoidal particles are indeed showing equilibrium shapes, we again annealed a suspension of the particles at 101 °C, above the  $T_g$  (78.0 °C) and  $T_{\text{cryst}}$  (98.6 °C) of PFO. After 40 s, the suspension was either quenched in liquid nitrogen or slowly cooled to room temperature. Figure 6 clearly shows that the PFO nanoparticles retain their significantly asymmetric ellipsoidal shape when heated above their  $T_g$ , when the chain mobility would be expected to allow the recovery of the spherical shape. This demonstrates again that the shape anisotropy is in thermal equilibrium and results from the underlying liquid crystalline order in the polymer chains.

## METHODS

### NANOPARTICLE SYNTHESIS

The main-chain polyether was provided by A.R.T. (Cavendish Laboratory). F8BT and PFO were purchased (ADS). The MCLCP nanoparticles were prepared as described previously<sup>16</sup>. The typical procedure is: 50 mg main-chain polyether is dissolved in 6.0 g chloroform and mixed with 10 g water containing 0.03 g SDS for pre-emulsification. After 5 min ultrasonication at 15% amplitude (Fisher company, Soniprep 150 with exponential microprobe) a stable mini-emulsion is produced. The sample is cooled in an ice box to prevent heating caused by the high-energy ultrasound. Evaporation of chloroform at 62 °C for 3 hours results in a stable suspension of polymer nanoparticles. Table 1 in the Supplementary Information lists the MCLCP nanoparticles that we prepared. The particle sizes are measured with a Malvern Zetasizer NanoZS.

### SEM CHARACTERIZATION

The particle suspension is deposited on a cleaned silicon wafer after 15–20 times dilution. SEM characterization is carried out on a field-emission LEO 1530 VP operating at 6 kV to image the morphology of nanoparticles. For all experiments, 50 particles in the SEM image are used to measure the particle size distribution. The shape change is observed using an SEM (Philips XL30 FEG) fitted with a cold stage CT1500 (Oxford Instruments). The heating speed is about 5 °C min<sup>-1</sup> during the whole process. The heating system is switched off during the imaging period to ensure that the system is stable, and to prevent the drift of the images at high temperatures.

Received 16 September 2004; accepted 22 March 2005; published 15 May 2005.

### References

- Donald, A. M. & Windle, A. H. *Liquid Crystalline Polymers* (Cambridge Univ. Press, Cambridge, 1992).
- Warner, M. & Terentjev, E. M. *Liquid Crystal Elastomers* (Clarendon, Oxford, 2003).
- Finkelmann, H., Nishikawa, E., Pereira, G. G. & Warner, M. A new opto-mechanical effect in solids. *Phys. Rev. Lett.* **87**, 015501 (2001).
- Küper, J. & Finkelmann, H. Liquid-crystal elastomers: influence of the orientational distribution of the crosslinks on the phase behaviour and reorientation processes. *Macromol. Chem. Phys.* **195**, 1353–1367 (1994).
- Joannopoulos, J. D., Villeneuve, P. R. & Fan, S. Photonic crystals: putting a new twist on light. *Nature* **386**, 143–149 (1997).
- Lu, Y., Yin, Y. & Xia, Y. Three-dimensional photonic crystals with non-spherical colloids as building blocks. *Adv. Mater.* **13**, 415–420 (2001).
- Xia, Y., Gates, B., Yin, Y. & Lu, Y. Monodispersed colloidal spheres: old materials with new applications. *Adv. Mater.* **12**, 693–713 (2000).
- Matijevic, E. Uniform inorganic colloid dispersions. Achievements and challenges. *Langmuir* **10**, 8–16 (1994).
- Morales, M. P., Gonzalez-Carreno, T. & Serna, C. J. The formation of  $\alpha\text{-Fe}_2\text{O}_3$  monodispersed particles in solution. *J. Mater. Res.* **7**, 2538–2545 (1992).
- van Dillen, T., van Blaaderen, A. & Polman, A. Shaping colloidal assemblies. *Mater. Today* **7**, 40–46 (2004).
- Jiang, P., Bertone, J. F. & Colvin, V. L. A lost-wax approach to monodisperse colloids and their crystals. *Science* **291**, 453–457 (2001).
- Ho, C. C., Keller, A., Odell, J. A. & Ottewill, R. H. Preparation of monodisperse ellipsoidal polystyrene particles. *Colloid Polym. Sci.* **271**, 469–479 (1993).
- Lu, Y., Yin, Y. & Xia, Y. Preparation and characterization of micrometer-sized 'egg shells'. *Adv. Mater.* **13**, 271–274 (2001).
- Percec, V. & Kawasumi, M. Liquid-crystalline polyethers based on conformational isomerism. 18. Polyethers based on a combined mesogenic unit containing rigid and flexible groups: 1-(4-hydroxy-4'-biphenyl)-2-(4-hydroxyphenyl)butane. *Macromolecules* **24**, 6318–6324 (1991).
- Grell, M., Bradley, D. D. C., Inbasekaran, M. & Woo, E. P. A glass-forming conjugated main-chain liquid crystal polymer for polarized electroluminescence applications. *Adv. Mater.* **9**, 798–802 (1997).
- Landfester, K. *et al.* Semiconducting polymer nanospheres in aqueous dispersion prepared by a miniemulsion process. *Adv. Mater.* **14**, 651–655 (2002).
- Ciferri, A., Krigbaum, W. R. & Meyer, R. B. *Polymer Liquid Crystals* (Academic, New York, 1982).
- Doi, M. & Edwards, S. F. *The Theory of Polymer Dynamics* (Clarendon, Oxford, 1986).
- Elias, F., Clarke, S. M., Peck, R. & Terentjev, E. M. Equilibrium textures in main-chain liquid crystalline polymers. *Europhys. Lett.* **47**, 442–448 (1999).
- Elias, F., Clarke, S. M., Peck, R. & Terentjev, E. M. Nematic order drives phase separation in polydisperse liquid crystalline polymers. *Macromolecules* **33**, 2060–2068 (2000).
- Landfester, K. Polyreactions in miniemulsions. *Macromol. Rapid Commun.* **22**, 896–936 (2001).
- Fridrikh, S. V. & Terentjev, E. M. Polydomain–monodomain transition in nematic elastomers. *Phys. Rev. E* **60**, 1847–1857 (1999).

### Acknowledgements

Z.Y. thanks the Overseas Research Studentship and Gates Cambridge Trust for financial support. Correspondence and requests for materials should be addressed to W.T.S.H. Supplementary Information accompanies the paper on [www.nature.com/naturematerials](http://www.nature.com/naturematerials).

### Competing financial interests

The authors declare that they have no competing financial interests.

Copyright of Nature Materials is the property of Nature Publishing Group. The copyright in an individual article may be maintained by the author in certain cases. Content may not be copied or emailed to multiple sites or posted to a listserv without the copyright holder's express written permission. However, users may print, download, or email articles for individual use.